A finite-deformation constitutive model of particle-binder composites incorporating yield-surface-free plasticity

Ankit Agarwal, Marcial Gonzalez

A finite-deformation constitutive model of particle-binder composites incorporating yield-surface-free plasticity

Ankit Agarwal[a,b], Marcial Gonzalez[a,b,*]

[a]*School of Mechanical Engineering, Purdue University, 585 Purdue Mall, West Lafayette, IN 47907, USA*
[b]*Ray W. Herrick Laboratories, Purdue University, 177 S Russel St, West Lafayette, IN 47907, USA*

Abstract

We present a quasi-static constitutive model for particle-binder composites which accounts for finite-deformation kinematics, non-linear elasto-plasticity without apparent yield, cyclic hysteresis and progressive stress-softening before the attainment of stable cyclic response. The model is based on deformation mechanisms experimentally observed during cyclic compression of Plastic-Bonded Explosives (PBX) at large strain. An additive decomposition of strain energy into elastic and inelastic parts is assumed, where the elastic response is modeled using Ogden hyperelasticity while the inelastic response is described using yield-surface-free endochronic plasticity based on the concepts of internal variables and of evolution or rate equations. Stress-softening is modeled using two approaches; a discontinuous isotropic damage model to appropriately describe the softening in the overall loading-unloading response, and a material scale function to describe the progressive cyclic softening until cyclic stabilization. Finally, a nonlinear multivariate optimization procedure is developed to estimate the elasto-plastic model parameters from nominal stress-strain experimental cyclic compression data, and a sensitivity analysis is conducted to quantify the influence of these parameters on the cyclic response.

Keywords: Elastic-plastic material (B), Constitutive behavior (B), Cyclic loading (B), Finite strain (B), Yield condition (A)

1. Introduction

Particle-binder composite materials consist of a large concentration of hard particles, called fillers, randomly dispersed in the matrix of a soft material. Generally, fillers are used to enhance the mechanical properties of the soft material. For example, filled elastomers such as carbon black and silica filled rubbers (Rattanasom et al., 2007; Omnès et al., 2008) have been shown to possess superior stiffness, strength and damping properties over natural rubber, making them suitable for application in automotive parts such as tires and bearing seals, and in structures providing vibration and shock isolation to mechanical systems.

Another class of particle-binder composites, called energetic composite materials or Plastic-Bonded Explosives (PBX), consists of explosive crystals and, in some formulations, metal fuel powder, embedded in a binder composed mainly of a soft polymer and a plasticizer. Since their initial development at Los Alamos National Laboratory in 1947, PBXs have been commonly used as ammunition in defense applications. Examples of explosives used include cyclotrimethylenetrinitramine (RDX) and cyclotetraminetetranitramine (HMX), while the binder composition includes polymers like hydroxyl-terminated polybutadiene (HTPB) and Estane, and plasticizers like Dioctyl adipate (DOA) and isodecyl pelargonate

*Corresponding author. Tel.: +1 765 494 0904; fax: +1 765 496 7537
Email addresses: agarwa80@purdue.edu (Ankit Agarwal), marcial-gonzalez@purdue.edu (Marcial Gonzalez)
URL: www.marcialgonzalez.net (Marcial Gonzalez)

(IDP), along with smaller concentrations of various additives (Akhavan, 2011). In PBX binder, the polymer, apart from providing structural integrity to the explosive, reduces their impact and vibrational sensitivity (Palmer et al., 1993; Rae et al., 2002; Rangaswamy et al., 2010), while the plasticizer improves their mechanical properties and processability (Yılmaz et al., 2014). The metal fuel, usually aluminum, is used to enhance the blast effects. Therefore, aluminized PBXs are typically used in naval weapons and missile warheads (Kumar et al., 2010).

Energetic composites are commonly used in applications requiring high mechanical confinement or compression (Wiegand, 2000; Wiegand & Reddingius, 2005). Additionally, these materials may be subjected to diverse loading conditions, ranging from low to high strain-rate cyclic, vibrational and impact loading during transport, storage and handling over their operational life. Since PBXs are designed to detonate under specific external energy stimulus, such loading conditions may alter their mechanical response, rendering them unpredictable and unsafe (Drodge & Williamson, 2016). Therefore, understanding and predicting the mechanical response of PBX under different loading conditions is of particular interest to the defense and propulsion community.

Earlier experimental studies on the mechanical behavior of PBX under uniaxial load have shown strong dependence on strain rate and temperature (Idar et al., 2002; Thompson et al., 2002; Williamson et al., 2008). Several constitutive models in the context of small and large deformation mechanics have been developed to model their rate and temperature-dependent behavior. For instance, Bardenhagen et al. (1998) proposed a large deformation viscoelastic model for PBX binder materials using Blatz-Ko hyperelasticity formulation and a Maxwell element. Clements & Mas (2001) proposed a viscoelastic constitutive theory for filled polymers using Boltzmann superposition principle, where the filler particles were modeled as randomly positioned elastic ellipsoidal particles. Composite stress relaxation functions were developed with their prony series coefficients dependent on filler concentration, ellipsoidal aspect ratio and polymer moduli. The visco-elastic cracking constitutive model developed by Bennett et al. (1998) combined a linear viscoelastic Maxwell's model with an isotropic damage model by Addessio & Johnson (1990). It was based on the mechanism of microcracking and derived from the statistical crack mechanics approach proposed by Dienes (1996) for brittle materials. The model was developed to predict the nonlinear stress-strain response of the material, as well as the strain-softening and nonlinearity observed due to extensive cracking at larger deformations. The model has since been extensively implemented in finite element analyses and used to predict the thermo-mechanical behavior of PBX and study hotspot generation (Rangaswamy et al., 2010; Buechler & Luscher, 2014). In the context of PBX undergoing low-frequency vibrational loading, nonlinear viscoelastic models for a mass-material system undergoing base excitation were proposed by Paripovic & Davies (2013, 2016).

While most of the constitutive formulations proposed for PBX model the material as viscoelastic due to the rubbery nature of the polymer binder, it has been shown that they can exhibit considerable plastic deformation with increasing confinement. Uniaxial confined compression tests carried out on inert mock sugar-based specimens for PBX 9501 (Wiegand, 2000; Wiegand & Reddingius, 2005) under different confining pressures revealed increasing plastic deformation and strain hardening with increasing pressure. Recently, Agarwal & Gonzalez (2020) conducted unconfined compression tests at room temperature and low strain rate (10^{-3}/s) on cylindrical specimens of three mock explosive formulations based on PBXN-109 (Lochert et al., 2002), with sugar as a substitute for the explosive HMX crystals. All three formulations contained 85% w/w of solids (sugar and aluminum), but differed from each other by the amount of aluminum content in the solids-composition, namely 85-00 (0% Al in solids, 0% in total), 85-15 (15% Al in solids, 12.75% in total) and 85-30 (30% additive in solids, 25.5% in total). The stress-strain response of the 85-00 specimens exhibited a quasi-brittle behavior (Pijaudier-Cabot et al., 1999), with an initial nonlinear increase in stress until a peak stress level at around 10-11% strain, followed by strain-softening due to evolution of microcracks into larger transgranular fracture leading to a loss of strength. Such behavior has been recorded and studied extensively for many non-aluminized PBX formulations (Idar et al., 1998, 2002;

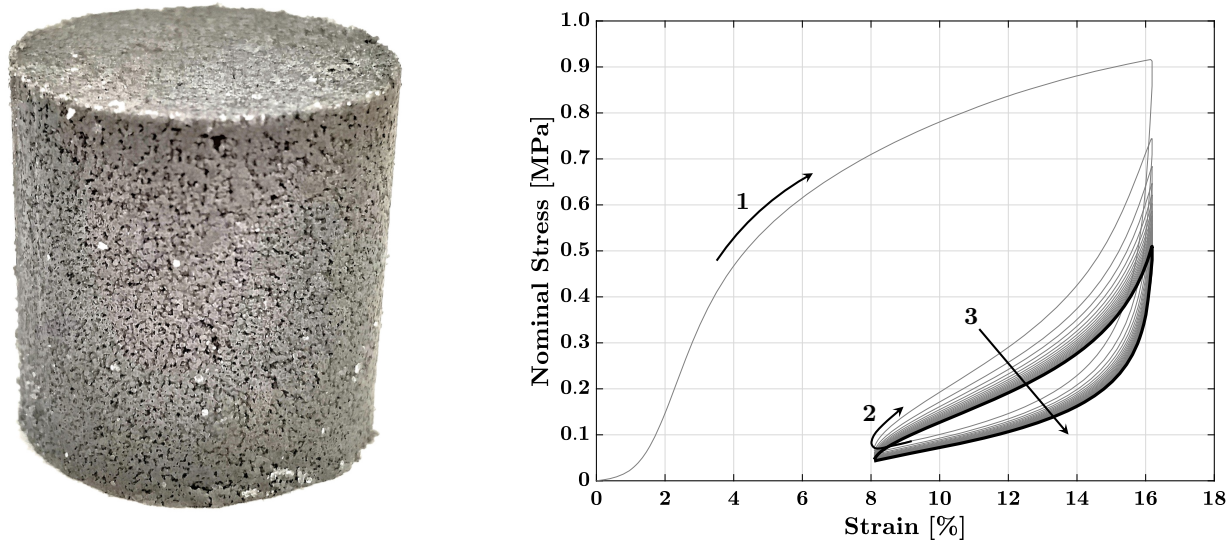

(a) (b)

Figure 1: (a) Aluminized mock sugar-based PBX specimen 85-15, and (b) the nominal stress-strain response under strain-controlled unconfined uniaxial compressive cyclic loading of the specimen. The response until the attainment of stable cyclic loop is shown in gray, while the stable cyclic loop is shown in black. Observable response attributes (labeled in the figure) include: (1) highly nonlinear stress-strain response without a distinctive yield point, (2) hysteresis, and (3) cyclic stress softening with eventual stabilization.

Rangaswamy et al., 2010). However, the aluminized specimens (i.e., 85-15 and 85-30 specimens) exhibited a more ductile plastic flow behavior with strain hardening, indicating that the presence of aluminum could cause the material to deform plastically even in the absence of confinement.

Additionally, plastic deformation and damage in PBX have been shown to be associated with hotspot mechanisms (Trumel, H. et al., 2012; Keyhani et al., 2019), thus directly impacting their ignition characteristics. Therefore, the development of a constitutive model capable of characterizing the plastic behavior of explosives is extremely important for proper modeling and prediction of their mechanical behavior. Constitutive models for PBX incorporating plasticity have been proposed for cyclic deformation (Le et al., 2010) and mild impact (Yang et al., 2018). However, the models have been developed using small deformation theory, and, therefore, are inapplicable to large deformation mechanical behavior of explosives.

Lastly, Agarwal & Gonzalez (2020) also conducted large deformation, unconfined cyclic compression tests of cylindrical sugar-based mock PBX specimens at room temperature and low strain rate (10^{-3}/s). Figure 1b shows the cyclic response of the 85-15 formulation. The strain-controlled, cyclic compression test was carried out by initially loading the specimen to 16% strain, and thereafter partially unloading-reloading between 8% and 16% strain. Observable response attributes (indicated in the figure) include: (1) a non-linear, continuous elasto-plastic response without apparent yield, (2) hysteresis, and (3) cyclic stress-softening with eventual stabilization. It is also worth noting that the curvature of the initial loading path is different from those of subsequent reloading paths. The former is convex and the latter are concave, indicating irreversible changes in the material behavior during the initial loading itself. This behavior has also been previously observed for cyclic compression of aluminized RDX-based PBX in HTPB binder (Tang et al., 2016).

The mechanical response of filled elastomers and PBX specimens exhibit similar characteristics at large deformations. Constitutive models of filled elastomers have been proposed adopting both phenomenological (see, e.g., Laiarinandrasana et al. (2003); Ayoub et al. (2014); Österlöf et al. (2016); Guo et al. (2018a,b)) and micromechanical (see, e.g., Dargazany et al. (2014); Raghunath et al. (2016); Plagge & Klüppel (2017)) frameworks. Ayoub et al. (2014) proposed a zener-type visco-hyperelastic constitutive

model of rubber-like materials that accounts for Mullins effect (Mullins, 1948, 1969), continuous stress-softening and permanent residual strains, utilizing the network alteration theory (Marckmann et al., 2002; Chagnon et al., 2006). Raghunath et al. (2016) extended the micromechanical dynamic flocculation model developed by Klüppel (2003) to include time-dependent effects typical of filled elastomers. The majority of these models attribute the observed hysteresis, and other inelastic phenomena, to time-dependent viscous overstress in the rubber matrix. In contrast, only a limited number of models consider these phenomena as time-independent plastic deformation mechanisms. A case in point is the phenomenological elasto-plastic constitutive model proposed by Kaliske & Rothert (1998) that captures the rate-independent process of internal material friction due to irreversible polymer slippage on the filler surface and plastic deformation of the filler particles. This multi-yield-surface rheological model is comprised of a finite number of elasto-plastic Prandtl elements arranged in parallel with an elastic member. More recently, yield-surface-free endochronic plasticity (Valanis, 1970) was utilized by Netzker et al. (2010) to model the smooth and hysteretic cyclic stress-strain response of carbon-black filled rubbers, with higher computational efficiency and less parameters.

In this paper, we present an elasto-plastic constitutive formulation with isotropic damage capable of modeling the cyclic response of mock energetic composite materials. Specifically, a Lagrangian finite-deformation formulation based on additive decomposition of strain energy (Simo, 1987; Govindjee & Simo, 1991; Holzapfel & Simo, 1996; Holzapfel, 1996, 2002) into elastic and plastic parts is adopted. The formulation uses Ogden's hyperelastic model (Ogden, 1972a,b) to predict the rubber-like nonlinear elastic response of the polymeric binder, and a hereditary (path-dependent) yield-surface-free endochronic plasticity theory (Valanis, 1970), based on the concept of internal state variables (Horstemeyer & Bammann, 2010), to account for irreversible deformations. A discontinuous isotropic damage model (Kachanov, 1986; Lemaitre et al., 1985) is utilized to model the stress-softening that occurs during unloading, and an endochronic material scale function (Valanis, 1970; Wu & Yip, 1981; Yeh, 1995; Lin et al., 2007) is utilized to model progressive cyclic stress softening and attainment of stable cyclic response. The number of model parameters is a function of the number of active Ogden terms and endochronic branches, and therefore a significant number of parameters may need to be identified. Therefore, we develop a parameter identification method based on a nonlinear multivariate least-squares problem, which is expected to be non-convex and affected by multiple local optima. The range of behavior predicted by the proposed model is demonstrated by calibrating parameters for the 85-15 formulation under cyclic compression (Agarwal & Gonzalez, 2020). Finally, to gain a better insight into the dependence of material response on model parameters, the analysis is concluded by studying the sensitivity of the cyclic compressive response to variations in the estimated values of endochronic and isotropic damage parameters.

The paper is organized as follows. The constitutive model is presented in Section 2, followed by Section 3 which provides a discrete numerical procedure to solve for stresses along a loading path. Section 4 presents the model parameter identification procedure and the calibrated material properties of the 85-15 mock PBX formulation. Section 5 shows a detailed sensitivity analysis of the yield-surface-free endochronic plasticity and the isotropic damage model. Finally, a summary and concluding remarks are presented in Section 6.

2. Constitutive model

2.1. General framework

The finite-deformation constitutive law is based on an additive decomposition of the Helmholtz free energy density function (Simo, 1987; Govindjee & Simo, 1991; Holzapfel & Simo, 1996; Holzapfel, 1996, 2002) into elastic and plastic parts and it employs a local multiplicative decomposition of the deformation gradient into isochoric and volumetric contributions. This approach is in contrast to the constitutive formulations based on multiplicative elastic-plastic decomposition of the deformation gradient (Kröner, 1959;

Lee & Liu, 1967; Lee, 1969; Gurtin & Anand, 2005) or additive decomposition of the rate of deformation tensor (Hill, 1950, 1958; Prager, 1961). For an isothermal elasto-plastic deformation process, the free energy density function Ψ is given by

$$\Psi(\mathbf{C}, \boldsymbol{\zeta}_1, \ldots, \boldsymbol{\zeta}_N) = \Psi^{\mathrm{e}}_{\mathrm{vol}}(J) + \Psi^{\mathrm{e}}_{\mathrm{iso}}(\bar{\mathbf{C}}) + \sum_{j=1}^{N} \Gamma^{\mathrm{i}}_j(\mathbf{C}, \boldsymbol{\zeta}_j) \tag{1}$$

where $\Psi^{\mathrm{e}}_{\mathrm{vol}}(J)$ and $\Psi^{\mathrm{e}}_{\mathrm{iso}}(\bar{\mathbf{C}})$ are the volumetric and isochoric elastic strain energy density functions, dependent respectively on the Jacobian of the deformation $J = \det(\mathbf{F})$ and on the isochoric right Cauchy-Green deformation tensor $\bar{\mathbf{C}} = \bar{\mathbf{F}}^T\bar{\mathbf{F}}$ (where $\bar{\mathbf{F}} = J^{-1/3}\mathbf{F}$). The inelastic strain energy $\sum_{j=1}^{N} \Gamma^{\mathrm{i}}_j(\mathbf{C}, \boldsymbol{\zeta}_j)$ is a set of configurational free energy functions Γ^{i}_j $(j = 1, \ldots, N)$ that characterizes the inelastic deformation behavior, namely irreversible slip at particle-particle and particle-binder contacts, plastic deformation and fracture of particles, among other dissipative mechanisms typical of particle-binder composites. The path-dependent dissipative potential dependents on the right Cauchy-Green deformation tensor $\mathbf{C}$ and a set of inelastic strain-like second-order tensorial internal variables $\boldsymbol{\zeta}_j$ $(j = 1, \ldots, N)$ that represent the inelastic deformation history of the material.

A discontinuous isotropic damage model is utilized to model the stress-softening that occurs during the unloading of particle-binder composites. For rubber or other polymeric materials, this phenomenon is known as Mullins effect (Mullins, 1948, 1969), and it has been phenomenologically described by applying a reduction factor of $(1 - D)$ to the stress of a hypothetical, undamaged material, where $D \in (0, 1]$ is the scalar damage variable (Kachanov, 1986; Lemaitre et al., 1985). Therefore, the second law of thermodynamics, in the form of the Clausius-Duhem inequality for an isothermal process, is given by

$$\mathcal{D}_{\mathrm{int}} := \frac{1}{2}\frac{\mathbf{S}}{1-D} : \dot{\mathbf{C}} - \dot{\Psi} = \frac{1}{2}\left[\frac{\mathbf{S}}{1-D} - 2\frac{\partial \Psi(\mathbf{C}, \boldsymbol{\zeta}_1, \ldots, \boldsymbol{\zeta}_N)}{\partial \mathbf{C}}\right] : \dot{\mathbf{C}} - \sum_{j=1}^{N} \frac{\partial \Gamma^{\mathrm{i}}_j(\mathbf{C}, \boldsymbol{\zeta}_j)}{\partial \boldsymbol{\zeta}_j} : \dot{\boldsymbol{\zeta}}_j \geq 0 \tag{2}$$

From standard arguments (Coleman & Noll, 1963; Coleman & Gurtin, 1967), the first term yields the definition of the second Piola-Kirchhoff stress, that is

$$\mathbf{S} = (1 - D)\, 2\frac{\partial \Psi(\mathbf{C}, \boldsymbol{\zeta}_1, \ldots, \boldsymbol{\zeta}_N)}{\partial \mathbf{C}} = (1 - D)\left[\mathbf{S}^{\mathrm{e}}_{\mathrm{vol}} + \mathbf{S}^{\mathrm{e}}_{\mathrm{iso}} + \sum_{j=1}^{N} \mathbf{S}^{\mathrm{i}}_j\right] \tag{3}$$

The second term results in a condition for each Γ^{i}_j, that is

$$\tilde{\mathbf{S}}^{\mathrm{i}}_j : \dot{\boldsymbol{\zeta}}_j \geq 0 \tag{4}$$

where the volumetric elastic stress $\mathbf{S}^{\mathrm{e}}_{\mathrm{vol}}$, the isochoric elastic stress $\mathbf{S}^{\mathrm{e}}_{\mathrm{iso}}$, the inelastic stress $\sum_{j=1}^{N} \mathbf{S}^{\mathrm{i}}_j$, and the stress-like internal variables $\tilde{\mathbf{S}}^{\mathrm{i}}_j$ (thermodynamically conjugate to $\boldsymbol{\zeta}_j$) are given by

$$\mathbf{S}^{\mathrm{e}}_{\mathrm{vol}} = J\frac{\mathrm{d}\Psi^{\mathrm{e}}_{\mathrm{vol}}(J)}{\mathrm{d}J}\mathbf{C}^{-1} \tag{5}$$

$$\mathbf{S}^{\mathrm{e}}_{\mathrm{iso}} = J^{-2/3}\mathrm{DEV}\left\{2\frac{\partial \Psi^{\mathrm{e}}_{\mathrm{iso}}(\bar{\mathbf{C}})}{\partial \bar{\mathbf{C}}}\right\} \tag{6}$$

$$\sum_{j=1}^{N} \mathbf{S}^{\mathrm{i}}_j = 2\sum_{j=1}^{N} \frac{\partial \Gamma^{\mathrm{i}}_j(\mathbf{C}, \boldsymbol{\zeta}_j)}{\partial \mathbf{C}} \tag{7}$$

$$\tilde{\mathbf{S}}^{\mathrm{i}}_j = -\frac{\partial \Psi}{\partial \boldsymbol{\zeta}_j} = -\frac{\partial \Gamma^{\mathrm{i}}_j(\mathbf{C}, \boldsymbol{\zeta}_j)}{\partial \boldsymbol{\zeta}_j} \qquad (j = 1, \ldots, N) \tag{8}$$

In the above equations, $\mathrm{DEV}\{\bullet\} = \{\bullet\} - (1/3)[\{\bullet\} : \mathbf{C}]\mathbf{C}^{-1}$ provides the deviator of a tensor in the reference configuration. It is worth noting that inequality (4) is satisfied by an evolution equation of the following form

$$\dot{\boldsymbol{\zeta}}_j = \mathbb{B}_j(\mathbf{C}, \boldsymbol{\zeta}_j) : \tilde{\mathbf{S}}^{\mathrm{i}}_j \tag{9}$$

where $\mathbb{B}_j$ is a positive definite fourth tensor (Holzapfel, 1996).

2.2. *Elastic strain energy*

The nonlinear elastic constitutive behavior of rubber-like materials, such as the binder in the application studied here, is commonly described through hyperelastic material models (see, e.g., the finite-deformations formulation presented by Mooney (1940); Rivlin (1948); Ogden (1972a,b); Boyce & Arruda (2000)). Ogden's hyperelastic model (Ogden, 1972a,b) is one of the most extensively used models for describing complex nonlinear responses, mainly due to its flexible series representation with the capability to introduce several model parameters. Specifically, the isochoric elastic strain energy density $\Psi^{\mathrm{e}}_{\mathrm{iso}}$ is given by

$$\Psi^{\mathrm{e}}_{\mathrm{iso}}(\bar{\mathbf{C}}) = \sum_{k=1}^{M} \frac{\mu_k}{\alpha_k}(\bar{\lambda}_1^{\alpha_k} + \bar{\lambda}_2^{\alpha_k} + \bar{\lambda}_3^{\alpha_k} - 3) \tag{10}$$

where the isochoric principle stretches are given by $\bar{\lambda}_a = J^{-1/3}\lambda_a$ $(a = 1, 2, 3)$ for principal stretches λ_a $(a = 1, 2, 3)$. Constants μ_k and α_k $(k = 1, \ldots, M)$ are material parameters that satisfy the following inequality to enforce stability in the material response

$$\mu_k \alpha_k > 0 \quad \forall\, k \in [1, M]\,, \tag{11}$$

From consistency conditions with respect to linear elasticity at small-strain (Ogden, 1984), the reference (ground-state) shear modulus of the material is given by

$$\mu = \sum_{k=1}^{M} \frac{\mu_k \alpha_k}{2} \tag{12}$$

2.3. *Discontinuous isotropic damage*

A discontinuous isotropic damage model (Kachanov, 1986; Lemaitre et al., 1985) is utilized to model the stress-softening that occurs during unloading, i.e., Mullins effect (Mullins, 1948, 1969) for polymeric materials, with scalar damage variable $D \in (0, 1]$. In the spirit of the damage function proposed by Zúñiga & Beatty (2002) and pseudoelastic damage functions proposed by Ogden & Roxburgh (1999) and Dorfmann & Ogden (2003), we specifically define the scalar damage variable as follows

$$D(\mathbf{C}, \phi^{\max}) = \tanh^{p}\left(\frac{\phi^{\max} - \phi(|\mathbf{C}|)}{m}\right) \tag{13}$$

where $\phi(|\mathbf{C}|)$ is the measure of deformation proposed by Beatty and co-workers (Beatty & Krishnaswamy, 2000; Zúñiga & Beatty, 2002) given by

$$\phi(|\mathbf{C}|) = |\mathbf{C}| = \sqrt{\mathbf{C} : \mathbf{C}} \tag{14}$$

and where $\phi^{\max}$ is the maximum deformation level given by

$$\phi^{\max}(t) = \max_{\tau \in [-\infty, t]} \phi(|\mathbf{C}(\tau)|) \tag{15}$$

The scalar damage variable is then a monotonic function of the deformation measure in the interval $\phi \in [\sqrt{3}, \phi^{\max}]$, with positive damage parameters m and p.

2.4. Yield-surface-free endochronic plasticity and evolution equation

As explained previously, particle-binder composites, specifically Plastic-Bonded Explosives (PBX), exhibit a non-linear elasto-plastic response without apparent yield. Classical plasticity theories require a yield surface and thus their applicability is limited for modeling these composites. In this study, we follow the work of Holzapfel & Simo (1996) and assume a quadratic relationship between free energy functions $\Gamma^{\mathrm{i}}_j(\mathbf{C}, \boldsymbol{\zeta}_j)$ and the internal variables $\boldsymbol{\zeta}_j$, i.e.

$$\frac{\partial \Gamma^{\mathrm{i}}_j}{\partial \boldsymbol{\zeta}_j \boldsymbol{\zeta}_k} = 2\mu_j \delta_{jk} \mathbb{I} \quad (j \text{ not summed}) \tag{16}$$

where μ_j are the reference (ground state) shear moduli related to j inelastic processes, δ_{mn} is the Kronecker delta and $\mathbb{I}$ is the fourth-order identity tensor. Therefore, by integrating eq. (16) twice, the following inelastic strain energy functions are obtained

$$\Gamma^{\mathrm{i}}_j(\mathbf{C}, \boldsymbol{\zeta}_j) = \mu_j |\boldsymbol{\zeta}_j|^2 + \mathbf{S}^*_j(\mathbf{C}) : \boldsymbol{\zeta}_j + \Psi^*_j(\mathbf{C}) \qquad (j = 1, \ldots, N) \tag{17}$$

where $\mathbf{S}^*(\mathbf{C})$ and $\Psi^*(\mathbf{C})$ are unknown tensor and scalar-valued functions, respectively. Similarly, an evolution or rate equation for the stress-like internal variables is obtained from eqs. (8), (9) and (17), and it is given by

$$\dot{\tilde{\mathbf{S}}}^{\mathrm{i}}_j + 2\mu_j \, \mathbb{B}_j(\mathbf{C}, \boldsymbol{\zeta}_j) : \tilde{\mathbf{S}}^{\mathrm{i}}_j = -\dot{\mathbf{S}}^*(\mathbf{C}) \qquad (j = 1, \ldots, N) \tag{18}$$

The inelastic strain energy without apparent yield is realized by adopting the endochronic plasticity theory developed by Valanis (1970). This theory is strain path-dependent in nature and it does not require the definition of a yield surface. This theory has been applied successfully to develop both infinitesimal-strain and finite-deformation plastic formulations to describe many metals and alloys (Wu & Yip, 1981; Valanis & Lee, 1984; Guo et al., 2016), concrete (Valanis & Read, 1986), powder compaction (Bakhshiani et al., 2002; Khoei et al., 2003; Khoei & Bakhshiani, 2004) and, more recently, filled elastomers (Netzker et al., 2010; Chen et al., 2018). In this work, we specifically assume

$$\mathbb{B}_j(\mathbf{C}, \boldsymbol{\zeta}_j) = \frac{\dot{z}(|\dot{\mathbf{C}}|)}{2\mu_j \gamma_j} \mathbb{I} \qquad (j = 1, \ldots, N) \tag{19}$$

where the intrinsic time scale z is a monotonically increasing measure of the deformation history, and the memory kernel is given by a set of positive dimensionless material parameters γ_j $(j = 1, \ldots, N)$ (see, for reference, Hsu et al. (1991) and Khoei et al. (2003)) that defines the path-dependent behavior of the formulation. It is worth noting that $\mu_j \gamma_j \geq 0$ for $\mathbb{B}_j$ to be a positive definite tensor. In addition, we assume

$$\mathbf{S}^*_j(\mathbf{C}) = -\mathbf{S}^{\mathrm{e}}_{\mathrm{iso},j}(\mathbf{C}) = -J^{-2/3} \mathrm{DEV} \left\{ 2 \frac{\partial \Psi^{\mathrm{e}}_{\mathrm{iso},j}(\bar{\mathbf{C}})}{\partial \bar{\mathbf{C}}} \right\} \qquad (j = 1, \ldots, N) \tag{20}$$

where $\Psi^{\mathrm{e}}_{\mathrm{iso},j}$ are a set of isochoric elastic strain energy functions defined according to the Ogden's model as

$$\Psi^{\mathrm{e}}_{\mathrm{iso},j} = \sum_{i=1}^{P} \frac{\mu_{ij}}{\alpha_{ij}} (\bar{\lambda}_1^{\alpha_{ij}} + \bar{\lambda}_2^{\alpha_{ij}} + \bar{\lambda}_3^{\alpha_{ij}} - 3) \qquad (j = 1, \ldots, N) \tag{21}$$

with constants μ_{ij} and α_{ij} such that $\mu_{ij}\alpha_{ij} > 0$ (cf. eq. (11)). It is worth noting that after substituting $\mathbb{B}_j$ and $\mathbf{S}^*_j$ according to eqs. (20) and (21) respectively, the evolution or rate equation (18) simplifies to

$$\dot{\tilde{\mathbf{S}}}^{\mathrm{i}}_j + \frac{\dot{z}(|\dot{\mathbf{C}}|)}{\gamma_j} \tilde{\mathbf{S}}^{\mathrm{i}}_j = \dot{\mathbf{S}}^{\mathrm{e}}_{\mathrm{iso},j} \qquad (j = 1, \ldots, N) \tag{22}$$

which can be regarded as the nonlinear extension of the one-dimensional isothermal evolution equation for a standard linear solid proposed by Valanis (1972) (see section 6 of the reference). Furthermore, by eliminating time dependence on both sides of differential equation and integrating with respect to the intrinsic time scale z, the classical hereditary or convolution form is recovered, that is

$$\tilde{\mathbf{S}}^{\mathrm{i}}_j = \tilde{\mathbf{S}}^{\mathrm{i}}_{j,0} + \int_0^z \dot{\mathbf{S}}^{\mathrm{e}}_{\mathrm{iso},j}\, \mathrm{e}^{-\frac{z-z'}{\gamma_j}}\, \mathrm{d}z' \qquad (j = 1, \ldots, N) \tag{23}$$

with $\tilde{\mathbf{S}}^{\mathrm{i}}_j(z = 0) = \tilde{\mathbf{S}}^{\mathrm{i}}_{j,0}$. Finally, for completeness, we set $\Psi^{*}_j(\mathbf{C}) = \Psi^{\mathrm{e}}_{\mathrm{iso},j}(\bar{\mathbf{C}})$ and, therefore, the reference shear moduli μ_j in (16) are given by

$$\mu_j = \sum_{i=1}^{P} \frac{\mu_{ij}\alpha_{ij}}{2} > 0 \qquad (j = 1, \ldots, N) \tag{24}$$

2.5. Intrinsic time scale and material scale function

The intrinsic time scale z, used in the evolution or rate equation (22) for internal variables $\tilde{\mathbf{S}}^{\mathrm{i}}_j$, is defined as

$$\dot{z}(|\dot{\mathbf{C}}|) = \frac{|\dot{\mathbf{C}}|}{f(z)} \tag{25}$$

where $f(z)$ is a material scale function that represents the transient cyclic behavior of the material until attainment of a stable response. In its simplest form, $f(z)$ is a monotonically increasing function for cyclic hardening materials, and a monotonically decreasing function for cyclic softening materials, that is asymptotic to a saturation value at steady state. A simple scale function proposed by Wu & Yip (1981) is given by

$$f(z) = c - (c-1)\mathrm{e}^{-\beta_c z} \tag{26}$$

where β_c controls the rate of evolution, and the value at steady state is $c > 1$, for hardening materials, and $c < 1$, for softening materials. Yeh (1995) and Lin et al. (2007) proposed the following improvements to the scale function

$$f(z) = \frac{c}{s-(s-1)\mathrm{e}^{-\beta_s z_{\mathrm{ref}}}} - \left(\frac{c}{s-(s-1)\mathrm{e}^{-\beta_s z_{\mathrm{ref}}}} - 1\right)\mathrm{e}^{-\beta_c (z - z_{\mathrm{ref}})} \tag{27}$$

In the above improved scale function, the additional parameter z_{ref}, defined as the value of z at which the last reversal of the strain path occurred, adds the capability to model "fading memory" effects exhibited by materials with memory (Coleman, 1964). In turn, the saturation value at steady state depends on the reference time scale z_{ref}. It is equal to c for $z_{\mathrm{ref}} = 0$, i.e., before the first reversal, and approaches c/s for $z_{\mathrm{ref}} \to \infty$, i.e., at cyclic stabilization. It is worth noting that for $c > s > 1$, the initial saturation value c is greater than the saturation value c/s at cyclic stabilization, i.e., the scale function describes the progressive cyclic softening typically observed in particle-binder composites. Figure 2 shows a schematic representation of the scale function proposed by Lin et al. (2007). It is evident from the figure that the rate of evolution of the material scale function is controlled by β_c, whereas the rate of evolution of the saturation value is controlled by β_s.

2.6. Inelastic stress

The inelastic stress $\mathbf{S}^{\mathrm{i}}_j$ is determined by using eq. (7) with the inelastic strain energy function defined by eq. (17) and by expressing the internal variable $\boldsymbol{\zeta}_j$ in terms of its conjugate $\tilde{\mathbf{S}}^{\mathrm{i}}_j$, i.e., using eq. (8). The result of this mathematical manipulation is given by

$$\mathbf{S}^{\mathrm{i}}_j = \mathbf{S}^{\mathrm{e}}_{\mathrm{iso},j} - \frac{1}{\mu_j}\frac{\partial \mathbf{S}^{\mathrm{e}}_{\mathrm{iso},j}}{\partial \mathbf{C}} : \left(\mathbf{S}^{\mathrm{e}}_{\mathrm{iso},j} - \tilde{\mathbf{S}}^{\mathrm{i}}_j\right) \tag{28}$$

where the internal variable $\tilde{\mathbf{S}}^{\mathrm{i}}_j$ is determined using the evolution or rate equation (22).

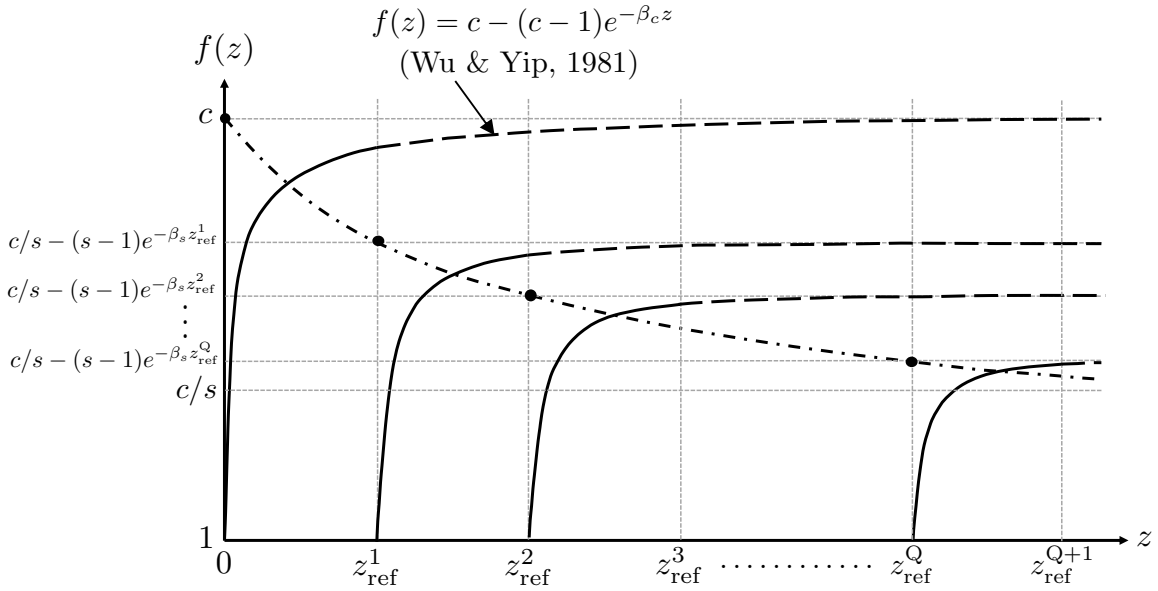

Figure 2: Schematic representation of the evolution of material scale function $f(z)$.

3. Incremental solution procedure

The constitutive model presented in the previous section is integrated by using an incremental solution procedure with time or loading intervals $[n, n+1]$. We assume that the state of the material, $\mathbf{C}_n$, $\tilde{\mathbf{S}}^{\text{i}}_{j,n}$, z_n, $z_{\text{ref},n}$, $\phi^{\max}_n$, is known at loading step n, and that $\mathbf{C}_{n+1}$ at loading step $n+1$ is given. The problem is then to determine $\tilde{\mathbf{S}}^{\text{i}}_{j,n+1}$, z_{n+1}, $z_{\text{ref},n+1}$, $\phi^{\max}_{n+1}$ at loading step $n+1$, and the value of the second Piola-Kirchhoff stress $\mathbf{S}_{n+1}$ which is given by

$$\mathbf{S}_{n+1} = (1 - D_{n+1})\left[\mathbf{S}^{\text{e}}_{\text{vol},n+1} + \mathbf{S}^{\text{e}}_{\text{iso},n+1} + \sum_{j=1}^{N} \mathbf{S}^{\text{e}}_{\text{iso},j,n+1} - \sum_{j=1}^{N} \frac{1}{2\mu_j} \bar{\mathbb{C}}_{j,n+1} : \left(\mathbf{S}^{\text{e}}_{\text{iso},j,n+1} - \tilde{\mathbf{S}}^{\text{i}}_{j,n+1}\right)\right] \tag{29}$$

where

$$\bar{\mathbb{C}}_{j,n+1} = 2\left[\frac{\partial \mathbf{S}^{\text{e}}_{\text{iso},j}}{\partial \mathbf{C}}\right]_{n+1} \tag{30}$$

$$\tilde{\mathbf{S}}^{\text{i}}_{j,n+1} = \frac{\left(1 - \Delta z/2\gamma_j\right)\tilde{\mathbf{S}}^{\text{i}}_{j,n} + \mathbf{S}^{\text{e}}_{\text{iso},j,n+1} - \mathbf{S}^{\text{e}}_{\text{iso},j,n}}{\left(1 + \Delta z/2\gamma_j\right)} \tag{31}$$

In the above equations, all quantities other than D_{n+1} and Δz are either known or depend on the right Cauchy-Green deformation tensor through equations (5), (6), and (20). The scalar damage variable D_{n+1} is computed after updating $\phi^{\max}_{n+1}$ using equation (15). The internal variable $\tilde{\mathbf{S}}^{\text{i}}_{j,n+1}$ defined by eq. (31) above is obtained by using a midpoint rule to discretize the evolution or rate equation (22), i.e., from

$$\tilde{\mathbf{S}}^{\text{i}}_{j,n+1} - \tilde{\mathbf{S}}^{\text{i}}_{j,n} + \left(\frac{\Delta z}{\gamma_j}\right)\left(\tilde{\mathbf{S}}^{\text{i}}_{j,n} + \frac{\tilde{\mathbf{S}}^{\text{i}}_{j,n+1} - \tilde{\mathbf{S}}^{\text{i}}_{j,n}}{2}\right) = \mathbf{S}^{\text{e}}_{\text{iso},j,n+1} - \mathbf{S}^{\text{e}}_{\text{iso},j,n} \tag{32}$$

The value of intrinsic time scale increment, Δz, is obtained by using a midpoint rule to discretize (25) together with (27), i.e., from

$$\Delta z\left[\frac{c}{s - (s-1)\mathrm{e}^{-\beta_s z_{\text{ref},n+1}}} - \left\{\frac{c}{s - (s-1)\mathrm{e}^{-\beta_s z_{\text{ref},n+1}}} - 1\right\}\mathrm{e}^{-\beta_c\left(z_n + \frac{\Delta z}{2} - z_{\text{ref},n+1}\right)}\right] - |\bar{\mathbf{C}}_{n+1} - \bar{\mathbf{C}}_n| = 0 \tag{33}$$

with $z_{n+1} = z_n + \Delta z$ and

$$z_{\text{ref},n+1} = \begin{cases} z_n & \text{if} \quad (\phi_{n+1} - \phi_n) \cdot (\phi_n - \phi_{n-1}) < 0 \\ z_{\text{ref},n} & \text{otherwise} \end{cases} \tag{34}$$

The above nonlinear equation is solved numerically using a Newton-Raphson method.

4. Model parameter identification of mock PBX

The range of behavior predicted by the proposed constitutive model is demonstrated by calibrating parameters for the 85-15 mock PBX formulation under cyclic compression (Agarwal & Gonzalez, 2020). Therefore, section 4.1 presents the incremental procedure for uniaxial cyclic loading under unconfined lateral conditions and incompressible material assumptions. Section 4.2 presents a parameter identification procedure based on a nonlinear multivariate minimization problem and the least-squares principle. Finally, sections 4.3 and 4.4 show the results of the parameter identification and the validation of the model, respectively.

4.1. Incremental procedure for uniaxial cyclic loading

The material is assumed to be incompressible, i.e., $J_n = 1$ and thus $\bar{\mathbf{C}}_n = \mathbf{C}_n$, due to the rubber-like behavior of the particle-binder composite. The cylindrical mock PBX specimen is loading along its axial direction which is coincidental with the $\mathbf{e}_3$ of a Cartesian coordinate system $\mathbf{e}_I$, with $I = 1, 2, 3$. Therefore, the right Cauchy-Green deformation tensor has principle stretches λ_I are related by

$$\lambda_{1,n} = \lambda_{2,n} = \frac{1}{\sqrt{\lambda_{3,n}}} \tag{35}$$

and principal directions aligned with the Cartesian axes, i.e., $\mathbf{C}_n = \sum_{I=1}^{3} \lambda_{I,n}^2 \mathbf{e}_I \otimes \mathbf{e}_I$. The specimen is laterally unconfined and the platens that apply the load are frictionless. Therefore, the only component of second Piola-Kirchhoff stress that is different from zero is $S_{33,n}$.

The elastic strain energy functions involved in the formulation reduce to

$$\begin{aligned} \Psi^{\text{e}}(\lambda_1, \lambda_2, \lambda_3) &= \sum_{k=1}^{M} \frac{\mu_k}{\alpha_k} (\lambda_1^{\alpha_k} + \lambda_2^{\alpha_k} + \lambda_3^{\alpha_k} - 3) \\ \Psi_j^{\text{e}}(\lambda_1, \lambda_2, \lambda_3) &= \sum_{i=1}^{P} \frac{\mu_{ij}}{\alpha_{ij}} (\lambda_1^{\alpha_{ij}} + \lambda_2^{\alpha_{ij}} + \lambda_3^{\alpha_{ij}} - 3) \qquad (j = 1, \ldots, N) \\ \Psi_{\text{vol}}^{\text{e}}(J) &= -p_o(J - 1) \end{aligned} \tag{36}$$

where the last term is used to augment the energy density and enforce the material internal or kinematic constraint imposed by incompressibility, i.e., $J = 1$, with p_o being the hydrostatic pressure.

Following the incremental procedure presented in section 3, we assume that the state of the material, $\mathbf{C}_n$, $\tilde{\mathbf{S}}_{j,n}^{\text{i}}$, z_n, $z_{\text{ref},n}$, $\phi_n^{\max}$, is known at loading step n, and that $\mathbf{C}_{n+1}$ at loading step $n+1$ is given. The maximum deformation level $\phi_{n+1}^{\max}$ is determined from (14) and (15) using

$$\phi_{n+1} = \sqrt{\lambda_{3,n+1}^4 + \frac{2}{\lambda_{3,n+1}^2}} \tag{37}$$

The intrinsic time scale increment Δz is obtained using (33) with

$$|\bar{\mathbf{C}}_{n+1} - \bar{\mathbf{C}}_n| = \sqrt{2\left(\lambda_{3,n+1}^{-1} - \lambda_{3,n}^{-1}\right)^2 + \left(\lambda_{3,n+1}^2 - \lambda_{3,n}^2\right)^2} \tag{38}$$

and $z_{\text{ref},n+1}$ is updated using (34) and $z_{n+1} = z_n + \Delta z$. The stress components in (29) simplify to

$$\begin{aligned}
S^{\text{e}}_{11,\text{iso},n+1} &= S^{\text{e}}_{22,\text{iso},n+1} = \sum_{k=1}^{M} \mu_k \lambda_{3,n+1}^{1-\alpha_k/2} \quad ; \quad S^{\text{e}}_{33,\text{iso},n+1} = \sum_{k=1}^{M} \mu_k \lambda_{3,n+1}^{\alpha_k-2} \\
S^{\text{e}}_{11,\text{vol},n+1} &= S^{\text{e}}_{22,\text{vol},n+1} = -p_{o,n+1}\lambda_{3,n+1} \quad ; \quad S^{\text{e}}_{33,\text{vol},n+1} = -p_{o,n+1}\lambda_{3,n+1}^{-2} \\
S^{\text{e}}_{11,\text{iso},j,n+1} &= S^{\text{e}}_{22,\text{iso},j,n+1} = \sum_{i=1}^{P} \mu_{ij} \lambda_{3,n+1}^{1-\alpha_{ij}/2} \quad ; \quad S^{\text{e}}_{33,\text{iso},j,n+1} = \sum_{i=1}^{P} \mu_{ij} \lambda_{3,n+1}^{\alpha_{ij}-2} \\
\bar{\mathbb{C}}_{1111,j,n+1} &= \bar{\mathbb{C}}_{2222,j,n+1} = \sum_{i=1}^{P} \mu_{ij}(\alpha_{ij}-2) \lambda_{3,n+1}^{2-\alpha_{ij}/2} \quad ; \quad \bar{\mathbb{C}}_{3333,j,n+1} = \sum_{i=1}^{P} \mu_{ij}(\alpha_{ij}-2) \lambda_{3,n+1}^{\alpha_{ij}-4}
\end{aligned} \tag{39}$$

where the hydrostatic pressure $p_{o,n+1}$ is obtained from the traction free boundary condition, i.e., from $S_{11,n+1} = S_{22,n+1} = 0$, using

$$p_{o,n+1} = \frac{1}{\lambda_{3,n+1}} \left[S^{\text{e}}_{11,\text{iso},n+1} + \sum_{j=1}^{N} S^{\text{e}}_{11,\text{iso},j,n+1} - \sum_{j=1}^{N} \frac{1}{2\mu_j} \bar{\mathbb{C}}_{1111,j,n+1} : \left(S^{\text{e}}_{11,\text{iso},j,n+1} - \tilde{S}^{\text{i}}_{11,j,n+1} \right) \right] \tag{40}$$

and the internal variable $\tilde{\mathbf{S}}^{\text{i}}_{j,n+1}$ is readily computed using eq. (31).

4.2. Parameter identification method

We have developed a parameter identification method based on a nonlinear multivariate minimization problem. The proposed constitutive model has $2M + 2P \times N + N + 6$ material parameters, namely

- $2M$ parameters in the elastic branch: μ_k and α_k ($k = 1, \ldots, M$).
- $2P \times N$ elastic parameters in the yield-surface-free endochronic branches: μ_{ij} and α_{ij} ($i = 1, \ldots, P$; $j = 1, \ldots, N$).
- N kernel parameters in the yield-surface-free endochronic branches: γ_j ($j = 1, \ldots, N$).
- 4 material scale function parameters: c, s, β_c and β_s.
- 2 isotropic damage parameters: m and p.

The method is based on the least-squares principle, for $\mathcal{N}$ experimental nominal stress values T_n^{exp} and corresponding model first Piola-Kirchhoff stress values $\lambda_{3,n} S_{33,n}$, and it is given by

$$\begin{aligned}
\min_{\mathbf{v} \in \mathbb{R}^{2M+2P\times N+N+6}, \epsilon_o} \quad & \frac{1}{\mathcal{N}} \sum_{n=1}^{\mathcal{N}} \left[T_n^{\text{exp}} - \lambda_{3,n} S_{33,n} \right]^2 \\
\text{subject to} \quad & -\mu_k \alpha_k \le 0 \quad \text{for} \;\; k = 1, \ldots, M \\
& -\mu_{ij} \alpha_{ij} \le 0 \quad \text{for} \;\; i = 1, \ldots, P; \; j = 1, \ldots, N \\
& s - c \le 0 \\
& \mathbf{v} \in [\mathbf{v}^{\min}, \mathbf{v}^{\max}]
\end{aligned} \tag{41}$$

where the inequality constraints come from Ogden's stability conditions (e.g., from equation (11) for the elastic branch), and from the requirement of progressive cyclic softening. Since the nonlinear optimization problem is expected to be non-convex and affected by multiple local optima, appropriate bounds are applied on the set of material parameters $\mathbf{v}$. Lastly, the experimental response of the mock PBX specimen suggests that the initial loading response is affected by machine/specimen mismatch (Figure 1b). Therefore, the initial part of the response is omitted from the parameter estimation by applying a strain offset ϵ_o to the experimental data and setting stresses for the initial mismatch to be zero.

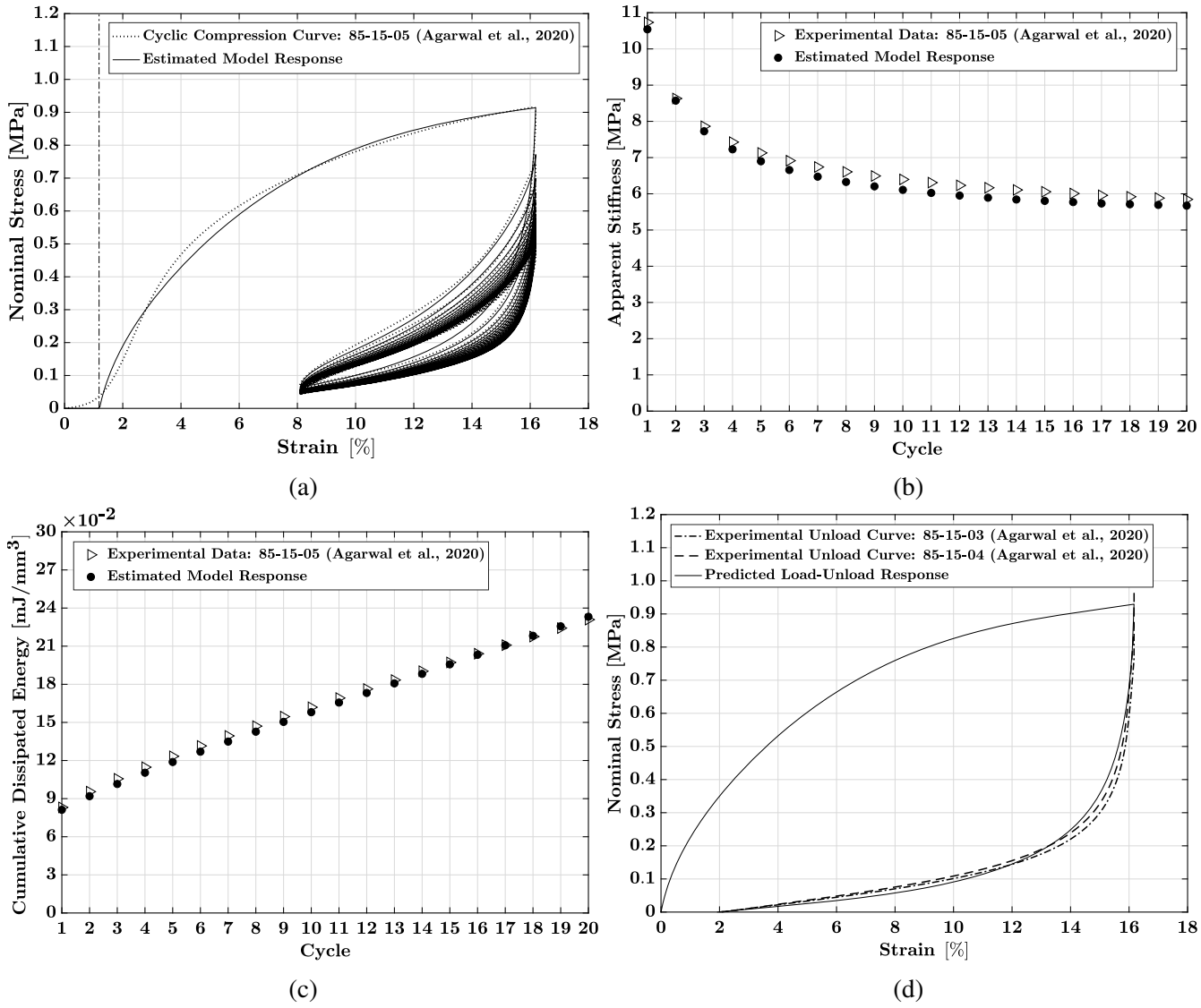

Figure 3: Experimental data and estimated model response for cyclic compression of the 85-15-05 PBX mock specimen, showing the (a) cyclic stress-strain curve, (b) evolution of apparent stiffness, and (c) cumulative energy dissipation with cyclic loading, and (d) the experimental and predicted model response of the unloading of specimens 85-15-03 and 85-15-04 from a strain level of 16%. The dashed-dotted line in (a) represents the value of machine/specimen mismatch offset ϵ_o.

4.3. Parameter identification of mock PBX

The nonlinear multivariate minimization problem presented above was solved in MATLAB®, Version 9.4.0 using the constrained optimization function *fmincon* with the default interior-point algorithm. The resulting estimated stress-strain curve, compared with the experimentally obtained response for the 85-15-05 specimen (ref. Agarwal & Gonzalez (2020) for the specific naming convention of the tested mock PBX specimens) is presented in Figure 3a, along with the experimental and model-estimated values of the apparent stiffness (Figure 3b) and of the cumulative energy dissipation (Figure 3c). The apparent stiffness is calculated as the slope of the line connecting peak and valley stresses in each cycle, while the cyclic energy dissipation is calculated as the difference between the energy supplied to the material (i.e., the area under the loading path) and the energy recovered after a cycle (i.e., the area under the unloading path). It is interesting to note that an excellent agreement between the experimental data and the model response is achieved with $M = 1$, $N = 3$ and $P = 1$. Therefore, the 85-15 mock formulation is well characterized by a total of 17 material parameters, listed in Table 1, with $\epsilon_o = 1.2\%$—shown in Figure 3a by a dashed-dotted vertical line.

Material properties of the 85-15 mock PBX formulation

Elastic branch ($M = 1$)

$\mu_1 = 1.4474$ MPa $\quad \alpha_1 = 10.4933$

Initial (ground-state) shear modulus $\mu^{\mathrm{e}} = \sum_{k=1}^{M} \mu_k \alpha_k / 2 = 7.5939$ MPa

Yield-surface-free endochronic branch 1 ($P = 1$)

$\mu_{11} = 13.5898$ MPa $\quad \alpha_{11} = 1.0454 \quad \gamma_1 = 0.0018$

Initial (ground-state) shear modulus $\mu_1^{\mathrm{i}} = \sum_{i=1}^{P} \mu_{i1} \alpha_{i1} / 2 = 7.1034$ MPa

Yield-surface-free endochronic branch 2 ($P = 1$)

$\mu_{12} = 1.2238$ MPa $\quad \alpha_{12} = 1.2841 \quad \gamma_2 = 0.0541$

Initial (ground-state) shear modulus $\mu_2^{\mathrm{i}} = \sum_{i=1}^{P} \mu_{i2} \alpha_{i2} / 2 = 0.7857$ MPa

Yield-surface-free endochronic branch 3 ($P = 1$)

$\mu_{13} = 0.5774$ MPa $\quad \alpha_{13} = 1.1829 \quad \gamma_3 = 0.4634$

Initial (ground-state) shear modulus $\mu_3^{\mathrm{i}} = \sum_{i=1}^{P} \mu_{i3} \alpha_{i3} / 2 = 0.3415$ MPa

Material scale function

$c = 11.1679 \quad s = 1.8178 \quad \beta_c = 423.9661 \quad \beta_s = 5.5234$

Isotropic damage

$m = 0.0764 \quad p = 0.6429$

Table 1: Material properties of the 85-15 mock PBX formulation with three yield-surface-free endochronic branches ($N = 3$).

4.4. Validation

A simple validation of the calibrated constitutive law under axial loading is performed using the unloading experimental response from a strain level of 16% to a stress-free state. Figure 3d shows very good agreement between the experimental unloading curves of specimens 85-15-03 and 85-15-04 (Agarwal & Gonzalez, 2020) and the model predictions. It is worth noting that while the unloading response remains fairly consistent from specimen-to-specimen, the loading response from a virgin state could vary considerably and, thus, it is not shown in the figure.

5. Sensitivity analysis of the yield-surface-free endochronic plasticity and the isotropic damage model

A sensitivity analysis of the cyclic stress-strain response to material properties of the yield-surface-free endochronic and the isotropic damage models is presented in this section. Specifically, we investigate the contribution of these material properties while keeping all other parameter values constant and equal to those obtained for the 85-15-05 mock PBX specimen.

5.1. Yield-surface-free endochronic plasticity

Figure 4 presents the influence of initial or ground-state shear moduli, i.e., μ_1 (Figure 4a), μ_2 (Figure 4c) and μ_3 (Figure 4e), and of kernel parameters, i.e., threshold strains γ_1 (Figure 4b), γ_2 (Figure 4d) and γ_3 (Figure 4f), on the stable cyclic response of the 85-15-05 mock PBX specimen. Solid curves correspond

to the response calibrated to experimental data, dashed-dotted curves show the effect of reduction in the parameter values, while dashed curves show the effect of increase in the parameter values. It is evident from the figures that increase (decrease) in the shear moduli μ_j significantly increases (decreases) the stiffness of the stress-strain response, while increase (decrease) in the threshold strains γ_j increases (decreases) the cyclic hysteresis energy. Additionally, the dominant contribution to these effects is from the first yield-surface-free endochronic branch, i.e., from parameters μ_1 and γ_1.

Figure 5 presents the influence of material scale function parameters c and s on the evolution of peak stress with cyclic compression of the 85-15 mock PBX specimen. It is evident from Figure 5a that variation in c results in almost proportional change in the magnitude of the peak stress of each cycle (see $f(z) \approx c$ and $f(z) \to c/s$ in figure 2). In contrast, variation in s does not change the peak stress for the first cycle but it has an almost inverse proportional effect on the magnitude of the peak stress upon cyclic stabilization. Similarly, figures 5b and 5c present the influence of material scale function parameters β_c and β_s on the evolution of peak stress. The main effect of increase (decrease) in the value of β_c is to increase (decrease) the magnitude of the peak stress of each cycle in a nonlinear fashion. In contrast, the main effect of increase (decrease) in the value of β_s is to decrease (increase) the magnitude of the peak stress upon cyclic stabilization in a nonlinear fashion. These nonlinearities result from the exponential term in equation (27).

5.2. Isotropic damage model

Figure 6 presents the influence of isotropic damage parameters m and p on the loading-unloading stress-strain response of the 85-15 mock PBX specimen. Both parameters control the stress-softening behavior during unloading. Specifically, an increase (decrease) in the values of m and p results in decreasing (increasing) softening. Specifically, the parameter m exerts a more significant influence on the amount of softening at low strain levels, while p has greater control over the softening at moderate-to-high strain levels.

6. Summary and discussion

We have presented a quasi-static constitutive model for particle-binder composites which accounts for finite-deformation kinematics, non-linear elasto-plasticity without apparent yield, cyclic hysteresis and progressive stress-softening before the attainment of stable cyclic response. The model is based on an additive decomposition of strain energy into elastic and inelastic parts, where the elastic response is modeled using Ogden hyperelasticity while the inelastic response is described using yield-surface free endochronic plasticity based on the concepts of internal variables and of evolution or rate equations. Stress-softening is modeled using two approaches; a discontinuous isotropic damage model to appropriately describe the overall softening between loading and unloading responses, and a material scale function to describe the progressive cyclic softening until attainment of stable response. The constitutive model is then based on the deformation mechanisms experimentally observed during cyclic compression of PBX at large strain.

Furthermore, we have proposed a discrete numerical procedure to solve for stresses along a loading path, and we have developed a parameter identification method, based on a nonlinear multivariate minimization problem, to determine material properties from experimental cyclic compression data. Specifically, we have used cyclic data for 85-15 mock PBX (Agarwal & Gonzalez, 2020) to demonstrate the range of behavior predicted by the proposed constitutive model and the effectiveness of the parameter identification method. This is evident from the remarkable model calibration results and validation against the unloading response from a strain level of 16% to a stress-free state. Finally, we have conducted a sensitivity analysis of the cyclic stress-strain response to material properties of yield-surface-free endochronic and the isotropic damage models.

We close by pointing out some limitations of our approach and possible directions for the future extension of our analysis. First, we have restricted our attention to quasi-static, i.e., low strain-rate behavior

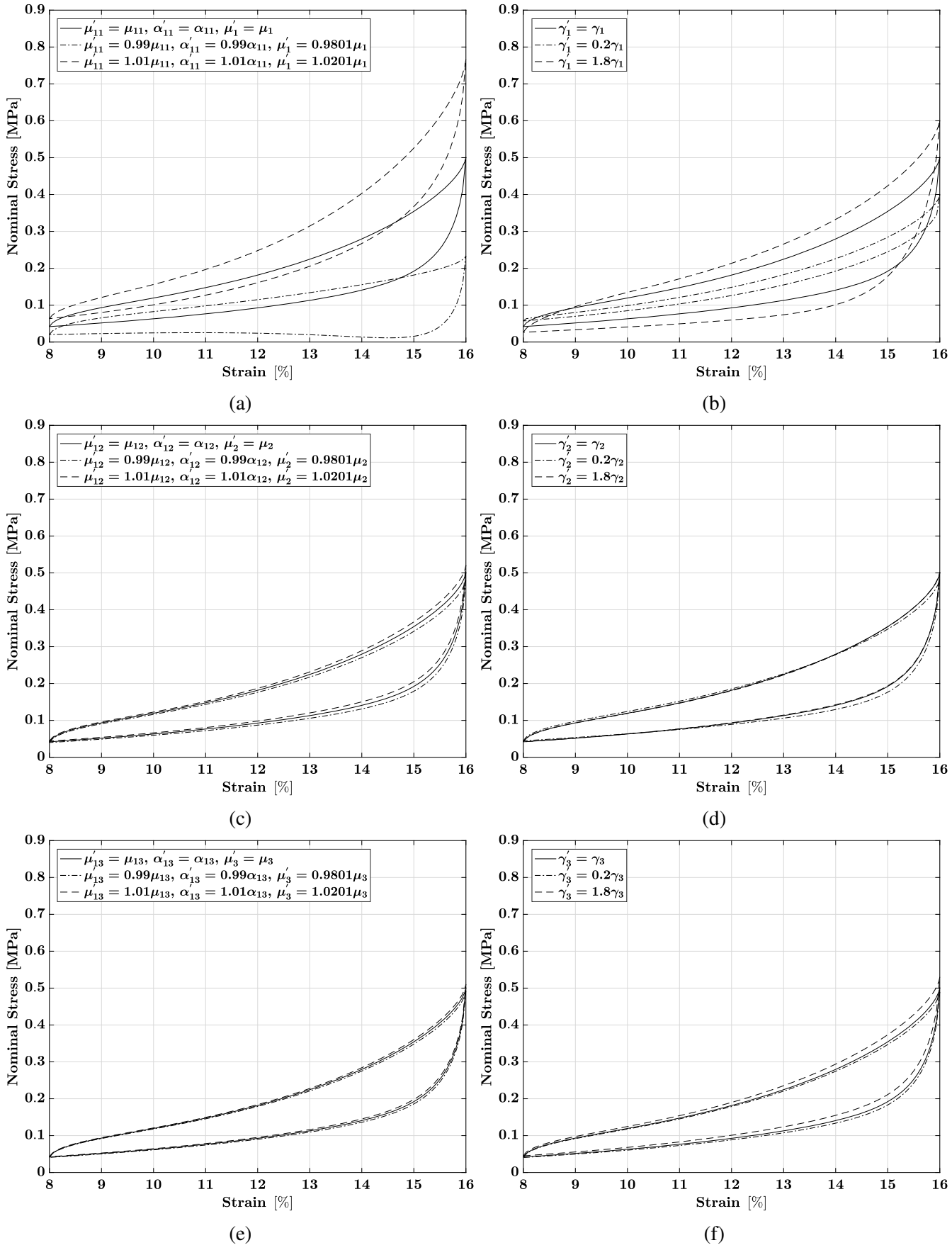

Figure 4: Stable cyclic response of the 85-15 mock PBX formulation for variations in yield-surface-free endochronic parameters (a) μ_1, (b) γ_1, (c) μ_2, (d) γ_2, (e) μ_3 and (f) γ_3.

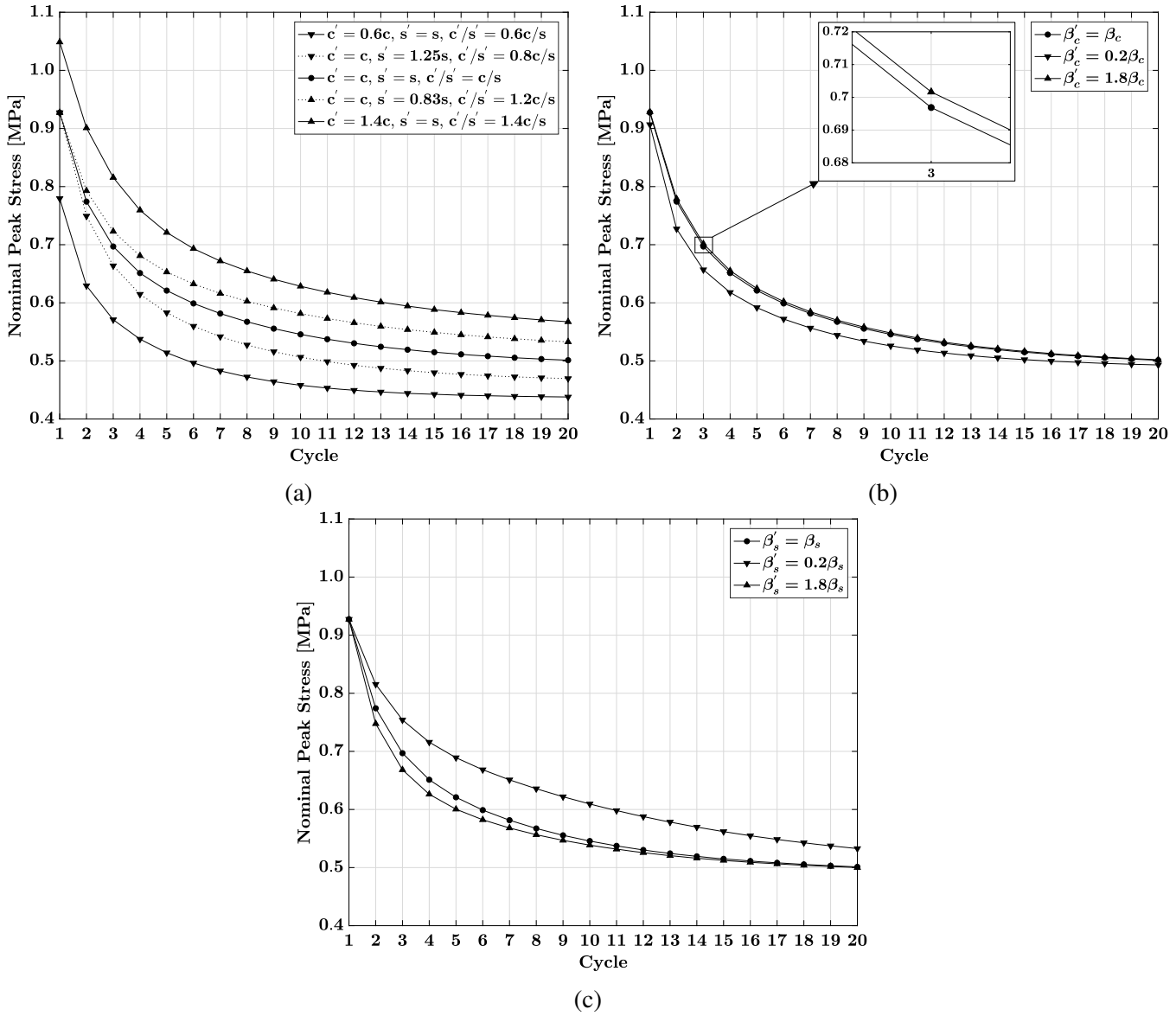

Figure 5: Cyclic peak stress of the 85-15 mock PBX formulation for variations in the material scale function parameters (a) c and s, (b) β_c and (c) β_s.

of particle-binder composites, and thereby neglected any strain-rate dependent effects in the constitutive model. However, it is well-known that viscous effects become dominant in these materials at moderate to high strain rates. Second, the proposed constitutive model carries an assumption of elasto-plastic incompressibility, which limits the analysis to particle-binder composites with moderate levels of compressibility. Therefore, the extension of the model to rate-dependent viscous effects and compressible behavior is a worthwhile direction of future research.

Acknowledgments

The authors wish to acknowledge Professor Patricia Davies, Professor Jeff Rhoads, Professor Steve Son, Professor Stuart Bolton, Jelena Paripovic, Allison Range, Nick Cummock, and Tim Manship for their feedback and interesting discussions.

This research is supported by the Air Force Research Laboratory through Grant No. FA8651-16-0287 entitled “Near-Resonant Thermomechanics of Energetic and Mock Energetic Composite Materials”,

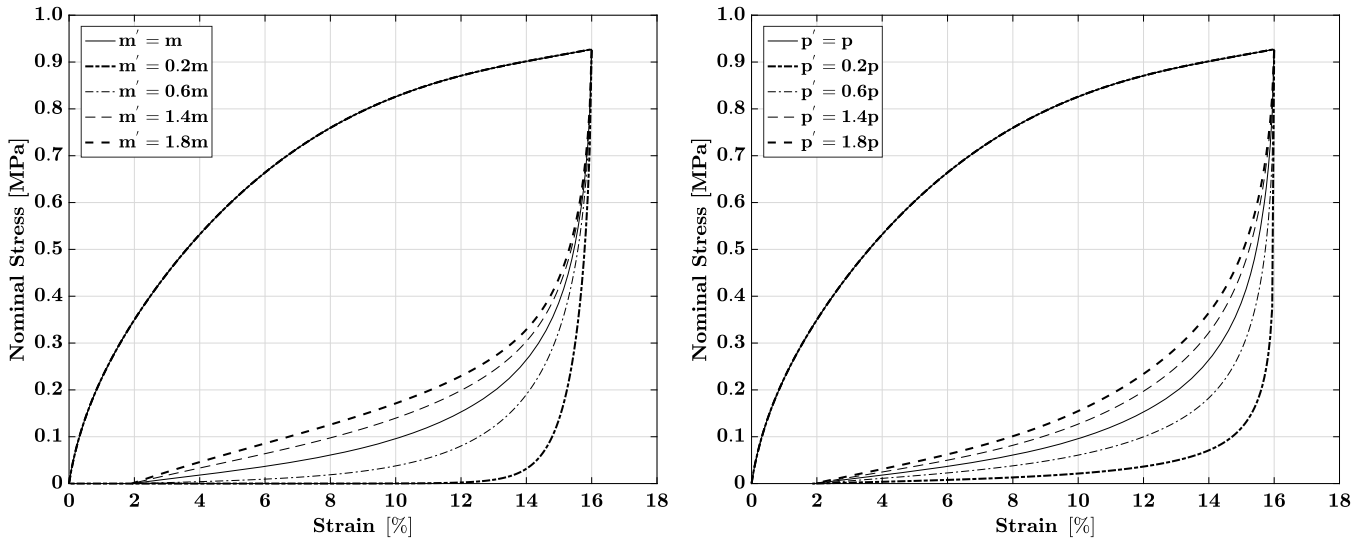

(a) (b)

Figure 6: Loading-unloading response of the 85-15 mock PBX formulation for variations in the isotropic damage parameters (a) m and (b) p.

Grant No. FA8651-16-D-0287 entitled "Near-Resonant Thermomechanics of Energetic and Mock Energetic Composite Materials, Part II", and Grant No. FA8651-17-S-0003 entitled "Exploring the Thermomechanics of Energetic and Mock Energetic Composite Materials Under Quasi-Static and Near-Resonant Excitations".

Distribution Statement A: Approved for public release. Distribution unlimited. (96TW-2020-0005)

References

Addessio, F. L., & Johnson, J. N. (1990). A constitutive model for the dynamic response of brittle materials. *Journal of Applied Physics*, *67*, 3275–3286. doi:10.1063/1.346090.

Agarwal, A., & Gonzalez, M. (2020). Effects of cyclic loading and time-recovery on microstructure and mechanical properties of particle-binder composites. *Journal of Applied Mechanics*, (pp. 1–39). doi:10.1115/1.4047038.

Akhavan, J. (2011). *Chemistry of Explosives*. (3rd ed.). Cambridge, UK: Royal Society of Chemistry.

Ayoub, G., Zaïri, F., Naït-Abdelaziz, M., Gloaguen, J., & Kridli, G. (2014). A visco-hyperelastic damage model for cyclic stress-softening, hysteresis and permanent set in rubber using the network alteration theory. *International Journal of Plasticity*, *54*, 19–33. doi:10.1016/j.ijplas.2013.08.001.

Bakhshiani, A., Khoei, A., & Mofid, M. (2002). An endochronic plasticity model for powder compaction processes. *Journal of materials processing technology*, *125*, 138–143. doi:10.1016/S0924-0136(02)00360-6.

Bardenhagen, S., Harstad, E., Maudlin, P., Gray, G., & Foster Jr, J. (1998). Viscoelastic models for explosive binder materials. In *AIP Conference Proceedings* (pp. 281–284). AIP volume 429. doi:10.1063/1.55647.

Beatty, M. F., & Krishnaswamy, S. (2000). A theory of stress-softening in incompressible isotropic materials. *Journal of the Mechanics and Physics of Solids*, *48*, 1931–1965. doi:10.1016/S0022-5096(99)00085-X.

Bennett, J. G., Haberman, K. S., Johnson, J. N., & Asay, B. W. (1998). A constitutive model for the non-shock ignition and mechanical response of high explosives. *Journal of the Mechanics and Physics of Solids*, *46*, 2303–2322. doi:10.1016/S0022-5096(98)00011-8.

Boyce, M. C., & Arruda, E. M. (2000). Constitutive models of rubber elasticity: a review. *Rubber chemistry and technology*, *73*, 504–523. doi:10.5254/1.3547602.

Buechler, M. A., & Luscher, D. J. (2014). A semi-implicit integration scheme for a combined viscoelastic-damage model of plastic bonded explosives. *International Journal for Numerical Methods in Engineering*, *99*, 54–78. doi:10.1002/nme.4672.

Chagnon, G., Verron, E., Marckmann, G., & Gornet, L. (2006). Development of new constitutive equations for the mullins effect in rubber using the network alteration theory. *International Journal of Solids and Structures*, *43*, 6817 – 6831. doi:https://doi.org/10.1016/j.ijsolstr.2006.02.011.

Chen, Y., Kang, G., Yuan, J., & Yu, C. (2018). Uniaxial ratchetting of filled rubber: Experiments and damage-coupled hyper-viscoelastic-plastic constitutive model. *Journal of Applied Mechanics*, *85*, 061013–061013–9. doi:10.1115/1.4039814.

Clements, B. E., & Mas, E. M. (2001). Dynamic mechanical behavior of filled polymers. I. Theoretical developments. *Journal of Applied Physics*, *90*, 5522–5534. doi:10.1063/1.1412843.

Coleman, B. D. (1964). Thermodynamics of materials with memory. *Archive for Rational Mechanics and Analysis*, *17*, 1–46. doi:10.1007/978-3-7091-2951-7.

Coleman, B. D., & Gurtin, M. E. (1967). Thermodynamics with internal state variables. *The Journal of Chemical Physics*, *47*, 597–613. doi:10.1063/1.1711937.

Coleman, B. D., & Noll, W. (1963). The thermodynamics of elastic materials with heat conduction and viscosity. *Archive for Rational Mechanics and Analysis*, *13*, 167–178. doi:10.1007/BF01262690.

Dargazany, R., Khiêm, V. N., & Itskov, M. (2014). A generalized network decomposition model for the quasi-static inelastic behavior of filled elastomers. *International Journal of Plasticity*, *63*, 94–109. doi:10.1016/j.ijplas.2013.12.004.

Dienes, J. K. (1996). A unified theory of flow, hot spots, and fragmentation with an application to explosive sensitivity. In L. Davison, D. E. Grady, & M. Shahinpoor (Eds.), *High-Pressure Shock Compression of Solids II: Dynamic Fracture and Fragmentation* (pp. 366–398). New York (NY), USA: Springer. doi:10.1007/978-1-4612-2320-7_14.

Dorfmann, A., & Ogden, R. (2003). A pseudo-elastic model for loading, partial unloading and reloading of particle-reinforced rubber. *International Journal of Solids and Structures*, *40*, 2699–2714. doi:10.1016/S0020-7683(03)00089-1.

Drodge, D. R., & Williamson, D. M. (2016). Understanding damage in polymer-bonded explosive composites. *Journal of Materials Science*, *51*, 668–679. doi:10.1007/s10853-013-7378-6.

Govindjee, S., & Simo, J. (1991). A micro-mechanically based continuum damage model for carbon black-filled rubbers incorporating mullins' effect. *Journal of the Mechanics and Physics of Solids*, *39*, 87–112. doi:10.1016/0022-5096(91)90032-J.

Guo, J., Wu, L., Yang, X., & Zhong, S. (2016). Elastic-plastic endochronic constitutive model of 0Crl7Ni4Cu4Nb stainless steels. *Mathematical Problems in Engineering*, *2016*. doi:10.1155/2016/4396296.

Guo, Q., Zaïri, F., & Guo, X. (2018a). A thermo-viscoelastic-damage constitutive model for cyclically loaded rubbers. Part I: Model formulation and numerical examples. *International Journal of Plasticity*, *101*, 106 – 124. doi:https://doi.org/10.1016/j.ijplas.2017.10.011.

Guo, Q., Zaïri, F., & Guo, X. (2018b). A thermo-viscoelastic-damage constitutive model for cyclically loaded rubbers. Part II: Experimental studies and parameter identification. *International Journal of Plasticity*, *101*, 58 – 73. doi:https://doi.org/10.1016/j.ijplas.2017.10.009.

Gurtin, M. E., & Anand, L. (2005). The decomposition $F=F^eF^p$, material symmetry, and plastic irrotationality for solids that are isotropic-viscoplastic or amorphous. *International Journal of Plasticity*, *21*, 1686–1719. doi:10.1016/j.ijplas.2004.11.007.

Hill, R. (1950). *The mathematical theory of plasticity*. Oxford engineering science series. Oxford, England: Clarendon Press.

Hill, R. (1958). A general theory of uniqueness and stability in elastic-plastic solids. *Journal of the Mechanics and Physics of Solids*, *6*, 236–249. doi:10.1016/0022-5096(58)90029-2.

Holzapfel, G. A. (1996). On large strain viscoelasticity: Continuum formulation and finite element applications to elastomeric structures. *International Journal for Numerical Methods in Engineering*, *39*, 3903–3926. doi:10.1002/(SICI)1097-0207(19961130)39:22<3903::AID-NME34>3.0.CO;2-C.

Holzapfel, G. A. (2002). Nonlinear solid mechanics: A continuum approach for engineering science. *Meccanica*, *37*, 489–490. doi:10.1023/A:1020843529530.

Holzapfel, G. A., & Simo, J. C. (1996). A new viscoelastic constitutive model for continuous media at finite thermomechanical changes. *International Journal of Solids and Structures*, *33*, 3019–3034. doi:10.1016/0020-7683(95)00263-4.

Horstemeyer, M. F., & Bammann, D. J. (2010). Historical review of internal state variable theory for inelasticity. *International Journal of Plasticity*, *26*, 1310–1334. doi:10.1016/j.ijplas.2010.06.005. Special Issue In Honor of David L. McDowell.

Hsu, S. Y., Jain, S. K., & Griffin, O. H. (1991). Verification of endochronic theory for nonproportional loading paths. *Journal of Engineering Mechanics*, *117*, 110–131. doi:10.1061/(ASCE)0733-9399(1991)117:1(110).

Idar, D., Peterson, P., Scott, P., & Funk, D. (1998). Low strain rate compression measurements of PBXN-9, PBX 9501, and mock 9501. In *AIP Conference Proceedings* (pp. 587–590). AIP volume 429. doi:10.1063/1.55704.

Idar, D. J., Thompson, D. G., Gray, G. T., Blumenthal, W. R., Cady, C. M., Peterson, P. D., Roemer, E. L., Wright, W. J., & Jacquez, B. J. (2002). Influence of polymer molecular weight, temperature, and strain rate on the mechanical properties of PBX 9501. In *AIP Conference Proceedings* (pp. 821–824). AIP volume 620. doi:10.1063/1.1483663.

Kachanov, L. M. (1986). *Introduction to continuum damage mechanics* volume 10 of *Mechanics of elastic stability*. Springer, Netherlands. doi:10.1007/978-94-017-1957-5.

Kaliske, M., & Rothert, H. (1998). Constitutive approach to rate-independent properties of filled elastomers. *International Journal of Solids and Structures*, *35*, 2057 – 2071. doi:https://doi.org/10.1016/S0020-7683(97)00182-0.

Keyhani, A., Kim, S., Horie, Y., & Zhou, M. (2019). Energy dissipation in polymer-bonded explosives with various levels of

constituent plasticity and internal friction. *Computational Materials Science*, *159*, 136 – 149. doi:https://doi.org/10.1016/j.commatsci.2018.12.008.

Khoei, A., & Bakhshiani, A. (2004). A hypoelasto-plastic finite strain simulation of powder compaction processes with density-dependent endochronic model. *International journal of solids and structures*, *41*, 6081–6110. doi:10.1016/j.ijsolstr.2004.05.013.

Khoei, A., Bakhshiani, A., & Mofid, M. (2003). An endochronic plasticity model for finite strain deformation of powder forming processes. *Finite Elements in Analysis and Design*, *40*, 187–211. doi:10.1016/S0168-874X(02)00223-8.

Klüppel, M. (2003). The role of disorder in filler reinforcement of elastomers on various length scales. In B. Capella, M. Geuss, M. Klüppel, M. Munz, E. Schulz, & H. Sturm (Eds.), *Filler-Reinforced Elastomers Scanning Force Microscopy* (pp. 1–86). Berlin, Heidelberg: Springer. doi:10.1007/b11054.

Kröner, E. (1959). Allgemeine kontinuumstheorie der versetzungen und eigenspannungen. *Archive for Rational Mechanics and Analysis*, *4*, 273–334. doi:10.1007/BF00281393.

Kumar, A., Rao, V., Sinha, R., & Rao, A. (2010). Evaluation of plastic bonded explosive (PBX) formulations based on RDX, aluminum, and HTPB for underwater applications. *Propellants, Explosives, Pyrotechnics*, *35*, 359–364. doi:10.1002/prep.200800048.

Laiarinandrasana, L., Piques, R., & Robisson, A. (2003). Visco-hyperelastic model with internal state variable coupled with discontinuous damage concept under total lagrangian formulation. *International Journal of Plasticity*, *19*, 977–1000. doi:10.1016/S0749-6419(02)00089-X.

Le, V. D., Gratton, M., Caliez, M., Frachon, A., & Picart, D. (2010). Experimental mechanical characterization of plastic-bonded explosives. *Journal of Materials Science*, *45*, 5802–5813. doi:10.1007/s10853-010-4655-5.

Lee, E., & Liu, D. (1967). Finite-strain elastic-plastic theory with application to plane-wave analysis. *Journal of Applied Physics*, *38*, 19–27. doi:10.1063/1.1708953.

Lee, E. H. (1969). Elastic-plastic deformation at finite strains. *Journal of Applied Mechanics*, *36*, 1–6. doi:10.1115/1.3564580.

Lemaitre, J., Chaboche, J.-L., & Germain, P. (1985). *Mécanique des matériaux solides* volume 2. Paris, France: Dunod.

Lin, H.-Y., Yeh, W.-C., & Lee, W.-J. (2007). A material function of endochronic theory and its application to test under axisymmetrically cyclic loading conditions. *Journal of Mechanics*, *23*, 135–148. doi:10.1017/S1727719100001167.

Lochert, I. J., Dexter, R. M., & Hamshere, B. L. (2002). *Evaluation of Australian RDX in PBXN-109*. Technical Report DSTO-TN-0440. Defence Science and Technology Organisation, Weapons Systems Division, Edinburgh (SA), Australia.

Marckmann, G., Verron, E., Gornet, L., Chagnon, G., Charrier, P., & Fort, P. (2002). A theory of network alteration for the mullins effect. *Journal of the Mechanics and Physics of Solids*, *50*, 2011 – 2028. doi:https://doi.org/10.1016/S0022-5096(01)00136-3.

MATLAB®, Version 9.4.0 (2018). Natick, Massachusetts: The MathWorks Inc., 1984–2018.

Mooney, M. (1940). A theory of large elastic deformation. *Journal of Applied Physics*, *11*, 582–592. doi:10.1063/1.1712836.

Mullins, L. (1948). Effect of stretching on the properties of rubber. *Rubber Chemistry and Technology*, *21*, 281–300. doi:10.5254/1.3546914.

Mullins, L. (1969). Softening of rubber by deformation. *Rubber Chemistry and Technology*, *42*, 339–362. doi:10.5254/1.3539210.

Netzker, C., Dal, H., & Kaliske, M. (2010). An endochronic plasticity formulation for filled rubber. *International Journal of Solids and Structures*, *47*, 2371–2379. doi:10.1016/j.ijsolstr.2010.04.026.

Ogden, R. W. (1972a). Large deformation isotropic elasticity – on the correlation of theory and experiment for incompressible rubberlike solids. *Proceedings of the Royal Society of London A: Mathematical, Physical and Engineering Sciences*, *326*, 565–584. doi:10.1098/rspa.1972.0026.

Ogden, R. W. (1972b). Large deformation isotropic elasticity: on the correlation of theory and experiment for compressible rubberlike solids. *Proceedings of the Royal Society of London A: Mathematical, Physical and Engineering Sciences*, *328*, 567–583. doi:10.1098/rspa.1972.0096.

Ogden, R. W. (1984). *Non-linear Elastic Deformations*. Mineola (NY), USA: Dover Publications.

Ogden, R. W., & Roxburgh, D. G. (1999). A pseudo–elastic model for the mullins effect in filled rubber. *Proceedings of the Royal Society of London A: Mathematical, Physical and Engineering Sciences*, *455*, 2861–2877. doi:10.1098/rspa.1999.0431.

Omnès, B., Thuillier, S., Pilvin, P., Grohens, Y., & Gillet, S. (2008). Effective properties of carbon black filled natural rubber: Experiments and modeling. *Composites Part A: Applied Science and Manufacturing*, *39*, 1141–1149. doi:10.1016/j.compositesa.2008.04.003.

Palmer, S. J. P., Field, J. E., & Huntley, J. M. (1993). Deformation, strengths and strains to failure of polymer bonded explosives. *Proceedings of the Royal Society of London. Series A: Mathematical and Physical Sciences*, *440*, 399–419. doi:10.1098/rspa.1993.0023.

Paripovic, J., & Davies, P. (2013). Identification of the dynamic behavior of surrogate explosive materials. In *International Design Engineering Technical Conferences and Computers and Information in Engineering Conference; 22nd Reliability, Stress*

Analysis, and Failure Prevention Conference; 25th Conference on Mechanical Vibration and Noise (p. V008T13A066). ASME volume 8. doi:10.1115/DETC2013-12755.

Paripovic, J., & Davies, P. (2016). A model identification technique to characterize the low frequency behaviour of surrogate explosive materials. *Journal of Physics: Conference Series*, *744*, 012124. doi:10.1088/1742-6596/744/1/012124.

Pijaudier-Cabot, G., Bittnar, Z., & Gérard, B. (1999). *Mechanics of quasi-brittle materials and structures*. Paris, France: Hermes Science Publications.

Plagge, J., & Klüppel, M. (2017). A physically based model of stress softening and hysteresis of filled rubber including rate- and temperature dependency. *International Journal of Plasticity*, *89*, 173 – 196. doi:https://doi.org/10.1016/j.ijplas.2016.11.010.

Prager, W. (1961). An elementary discussion of definitions of stress rate. *Quarterly of Applied Mathematics*, *18*, 403–407.

Rae, P. J., Goldrein, H. T., Palmer, S. J. P., Field, J. E., & Lewis, A. L. (2002). Quasi-static studies of the deformation and failure of β-HMX based polymer bonded explosives. *Proceedings of the Royal Society of London. Series A: Mathematical, Physical and Engineering Sciences*, *458*, 743–762. doi:10.1098/rspa.2001.0894.

Raghunath, R., Juhre, D., & Klüppel, M. (2016). A physically motivated model for filled elastomers including strain rate and amplitude dependency in finite viscoelasticity. *International Journal of Plasticity*, *78*, 223–241. doi:10.1016/j.ijplas.2015.11.005.

Rangaswamy, P., Thompson, D. G., Liu, C., & Lewis, M. W. (2010). Modeling the mechanical response of PBX 9501. In *Proceedings of the 14th International Detonation Symposium* (pp. 174–183). Coeur d'Alene (ID), USA.

Rattanasom, N., Saowapark, T., & Deeprasertkul, C. (2007). Reinforcement of natural rubber with silica/carbon black hybrid filler. *Polymer Testing*, *26*, 369–377. doi:10.1016/j.polymertesting.2006.12.003.

Rivlin, R. (1948). Large elastic deformations of isotropic materials IV. Further developments of the general theory. *Philosophical Transactions of the Royal Society A*, *241*, 379–397. doi:10.1098/rsta.1948.0024.

Simo, J. (1987). On a fully three-dimensional finite-strain viscoelastic damage model: Formulation and computational aspects. *Computer Methods in Applied Mechanics and Engineering*, *60*, 153–173. doi:10.1016/0045-7825(87)90107-1.

Österlöf, R., Wentzel, H., & Kari, L. (2016). A finite strain viscoplastic constitutive model for rubber with reinforcing fillers. *International Journal of Plasticity*, *87*, 1 – 14. doi:https://doi.org/10.1016/j.ijplas.2016.08.008.

Tang, M.-f., Pang, H.-y., Lan, L.-g., Wen, M.-p., & Ming, L. (2016). Constitutive behavior of RDX-based PBX with loading-history and loading-rate effects. *Chinese Journal of Energetic Materials*, *24*, 832–837. doi:10.11943/j.issn.1006-9941.2016.09.002.

Thompson, D. G., Idar, D. J., Gray, G., Blumenthal, W. R., Cady, C. M., Roemer, E. L., Wright, W. J., & Peterson, P. D. (2002). Quasi-static and dynamic mechanical properties of new and virtually-aged PBX 9501 composites as a function of temperature and strain rate. In *Proceedings of the 12th International Detonation Symposium* (pp. 363–368). San Diego (CA), USA.

Trumel, H., Lambert, P., & Biessy, M. (2012). Mechanical and microstructural characterization of a HMX-based pressed explosive: Effects of combined high pressure and strain rate. *EPJ Web of Conferences*, *26*, 02005. doi:10.1051/epjconf/20122602005.

Valanis, K., & Read, H. (1986). An endochronic plasticity theory for concrete. *Mechanics of Materials*, *5*, 277–295. doi:10.1016/0167-6636(86)90024-4.

Valanis, K. C. (1970). *A theory of viscoplasticity without a yield surface part 1 - general theory*. Technical Report AFOSR-71-1765. Air Force Office of Scientific Research, Office of Aerospace Research, US Air Force, Arlington (VA), USA.

Valanis, K. C. (1972). *Irreversible thermodynamics of continuous media: internal variable theory* volume 77 of *International Centre for Mechanical Sciences book series*. Springer, Vienna. doi:10.1007/978-3-7091-2987-6.

Valanis, K. C., & Lee, C. (1984). Endochronic theory of cyclic plasticity with applications. *Journal of Applied Mechanics*, *51*, 367–374. doi:10.1115/1.3167627.

Wiegand, D. A. (2000). The influence of confinement on the mechanical properties of energetic materials. In *AIP Conference Proceedings* (pp. 675–678). AIP volume 505. doi:10.1063/1.1303563.

Wiegand, D. A., & Reddingius, B. (2005). Mechanical properties of confined explosives. *Journal of Energetic Materials*, *23*, 75–98. doi:10.1080/07370650590936415.

Williamson, D. M., Siviour, C. R., Proud, W. G., Palmer, S. J. P., Govier, R., Ellis, K., Blackwell, P., & Leppard, C. (2008). Temperature-time response of a polymer bonded explosive in compression (EDC37). *Journal of Physics D: Applied Physics*, *41*, 085404. doi:10.1088/0022-3727/41/8/085404.

Wu, H., & Yip, M. (1981). Endochronic description of cyclic hardening behavior for metallic materials. *Journal of Engineering Materials and Technology*, *103*, 212–217. doi:10.1115/1.3225003.

Yang, K., Wu, Y., & Huang, F. (2018). Numerical simulations of microcrack-related damage and ignition behavior of mild-impacted polymer bonded explosives. *Journal of Hazardous Materials*, *356*, 34–52. doi:10.1016/j.jhazmat.2018.05.029.

Yeh, W.-C. (1995). Verification of the endochronic theory of plasticity under biaxial load. *Journal of the Chinese Institute of Engineers*, *18*, 25–34. doi:10.1080/02533839.1995.9677663.

Yılmaz, G. A., Şen, D., Kaya, Z. T., & Tinçer, T. (2014). Effect of inert plasticizers on mechanical, thermal, and sensitivity properties of polyurethane-based plastic bonded explosives. *Journal of Applied Polymer Science*, *131*. doi:10.1002/app.40907.

Zúñiga, A. E., & Beatty, M. F. (2002). A new phenomenological model for stress-softening in elastomers. *Zeitschrift für angewandte Mathematik und Physik ZAMP*, *53*, 794–814. doi:10.1007/PL00022513.